A Review of the Systems Approach to the Analysis of Dynamic-Mode Atomic Force Microscopy

Abu Sebastian, *Member, IEEE*, Anil Gannepalli, and Murti V. Salapaka, *Member, IEEE*

***Abstract*—The atomic force microscope (AFM) is one of the foremost tools for imaging, measuring and manipulating matter at the nanoscale. This brief presents a review of the systems and control approach to analyzing the challenging dynamic-mode operation of the AFM. A Luré system perspective of the AFM dynamics facilitates the application of powerful tools from systems theory for the analysis. The harmonic balance method provides significant insights into the steady-state behavior as well as a framework for identifying the tip-sample interaction force. A simple piecewise-linear tip-sample interaction model and its identification using the harmonic balance method is presented. The dominant first harmonic is analyzed using multivalued frequency responses and the corresponding stability conditions. The ability of the simple tip-sample interaction model to capture the intricate nonlinear behavior of the first harmonic is demonstrated. This also points to the importance of studying the higher harmonics to obtain finer details of the tip-sample interaction. The suitability of the Luré system perspective for the analysis of the higher harmonics is demonstrated.**

***Index Terms*—Asymptotic methods, atomic force microscopy (AFM), dynamic-mode AFM, harmonic balance, integral quadratic constraints, Luré system.**

I. Introduction

In 1986, Binnig, Quate, and Gerber invented the atomic force microscope (AFM) to investigate surfaces of insulators at the atomic scale in a noninvasive manner [1]. The primary component of an AFM is a microcantilever, which is supported at one end and has a sharp tip at the other end for probing the sample surface (see Fig. 1). The cantilever forms a force probe that deflects owing to the interaction force between the tip and the sample. The force on the cantilever probe depends on the position of the tip. When the tip is far away from the sample, the interaction force is minimal. As the tip is brought closer, the cantilever starts experiencing relatively weak attractive forces and on further approach to the sample, the interaction force starts becoming repulsive in nature [2].

In the traditional contact-mode operation, the tip probes the repulsive regime of the interaction force. The tip is said to be "in contact" with the sample. The deflection of the cantilever due to the tip sample interaction force is monitored to infer sample properties. This mode of operation is rather harsh on the sample and hence not suitable for numerous applications. In the dynamic-mode operation, the cantilever is made to oscillate by an external forcing signal (see Fig. 2). The oscillating cantilever tip traverses a wide range of the interaction potential, probing the attractive and possibly repulsive regimes of the tip sample interaction forces intermittently. Dynamic-mode operations where the tip probes the repulse regime are typically referred to as tapping mode in AFM literature. Owing to this intermittent nature of the interaction with the sample, this mode of operation leads to much smaller lateral and vertical forces. The changes in the cantilever oscillation due to the tip sample interaction are monitored to infer sample properties. Because of its gentle nature, dynamic-mode operation is the preferred mode of operation for biological investigation.

One of the applications of the AFM and in particular of dynamic-mode AFM, is the reconstruction of the tip sample force profile. In this application, the cantilever sample offset is varied with respect to the oscillating cantilever. The cantilever oscillation and its relationship to the cantilever sample offset are analyzed to obtain the tip sample force profile. Throughout this operation, the sample is maintained at the same lateral position.

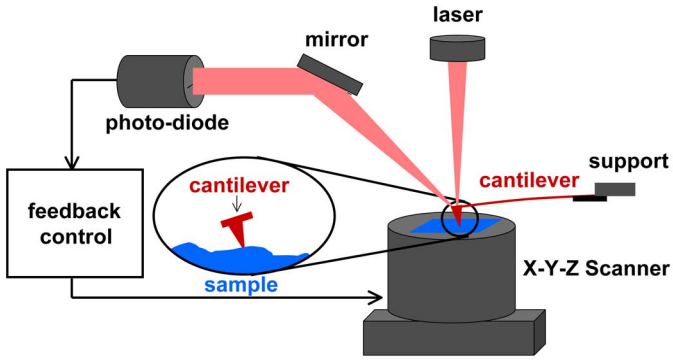

Fig. 1. Schematic of a typical AFM.

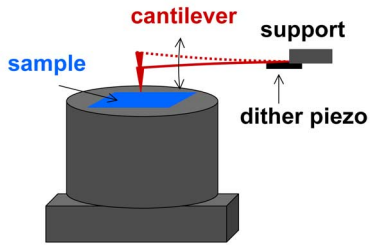

Fig. 2. Schematic depicting the microcantilever during dynamic-mode operation of the AFM.

Manuscript received February 19, 2007. Manuscript received in final form April 20, 2007. Recommended by Guest Editor S. Devasia. The work of M. Salapaka was supported by the National Science Foundation under Grant CMS 0626171 and Grant ECS 0601571.

A. Sebastian is with IBM Research GmbH, Zurich Research Laboratory, 8803 Rüschlikon, Switzerland (e-mail: ase@zurich.ibm.com).

A. Gannepalli is with Asylum Research Inc., Santa Barbara, CA 93117 USA (e-mail: ganil@rasy.com).

M. V. Salapaka is with the Department of Electrical and Computer Engineering, Iowa State University, Ames, IA 50011 USA (e-mail: murti@iastate.edu).

Color versions of one or more of the figures in this paper are available online at http://ieeexplore.ieee.org.

Digital Object Identifier 10.1109/TCST.2007.902959

However, in the more prevalent use, the sample is moved laterally. As the sample is moved laterally, the sample topography modulates the cantilever sample offset. The subsequent changes to the cantilever oscillation thus form a basis for imaging the topography of the sample. Note that understanding the tip sample force profile is crucial to the task of imaging the sample topography as the sample is positioned laterally. Typically, a set point property of the oscillating cantilever (e.g., the amplitude of the first harmonic) is regulated using a feedback controller that moves the sample vertically relative to the cantilever. A piezoelectric scanner is typically employed to position the sample relative to the cantilever in the lateral and the vertical direction. Thus, estimation of the tip sample force profile and topographic imaging are two of the primary applications of dynamic-mode AFM, both of which require a detailed understanding of how the cantilever and its tip interact with the sample.

The dynamic-mode operation of the AFM is particularly challenging because the tip traverses a long range of highly nonlinear tip sample interaction potential. The complexity of the dynamics is demonstrated by the experimental and theoretical studies that confirm the existence of chaotic behavior under certain operating conditions [3], [4]. Another indication is the experimentally observed feature that the cantilever can settle into two different stable trajectories for the same cantilever sample offset. Systems and control perspectives have significantly contributed to the analysis of dynamic-mode AFM and to the development of novel modes of imaging [5]–[7]. This brief provides a review of the systems and control approach to the analysis of dynamic-mode operation. Hereby the analysis of dynamic-mode AFM is greatly facilitated by casting the tip sample dynamics as an interconnection of a linear system that models the cantilever with a nonlinear system that models the tip sample interaction forces. This perspective of a Luré system was introduced in [8]. Further advances in the systems viewpoint-based analysis of AFM dynamics and its applications are presented in [9]–[12].

The Luré system perspective facilitates the application of powerful tools from systems theory to the analysis of dynamic-mode operation. The harmonic balance method constitutes one of the main tools. The resulting harmonic balance equations provide significant insights into the steady-state behavior of the cantilever oscillation. They also provide a framework for the systematic identification of tip sample force profile. The identification of a piecewise linear tip- sample interaction model is illustrated. This representative and tractable model can effectively be used to simulate the dynamic-mode AFM, which can aid controller design and provide insights into the AFM dynamics without carrying out extensive experiments.

The Luré perspective and experiments show the dominance of the first harmonic of the cantilever oscillations. Experiments indicate a multivalued dependence of the first harmonic on the sample topography. Thus, the analysis of the first harmonic, which is the main signal used for imaging, assumes particular importance. In this brief, we present the application of asymptotic methods, pioneered by Bogoliubov [13], to the analysis of the first harmonic of the microcantilever oscillation assuming a piecewise linear model of the tip sample interaction force. Some of the significant analytical and numerical investigations that have helped understand the behavior of the first harmonic are reported in [8] and [14]–[19].

An important insight obtained by the study of the first harmonic is that a simple piecewise linear model is capable of reproducing most of the intricate experimentally observed features further reinforcing the importance of studying the higher harmonics for the possibility of extracting further information on the tip sample interaction potential.

This brief is organized as follows. In Section II, the Luré system perspective of the cantilever sample system is introduced. The harmonic balance method is presented in Section III. In Section IV, the analysis of the dominant first harmonic along with the piecewise linear tip sample interaction model is presented. The review concludes with a discussion on the analysis of the higher harmonics using the systems perspective presented in Section V.

II. Luré System Perspective of the Cantilever Sample System

In spite of the popularity of the dynamic-mode operation, several experimental features were not well understood for many years. When the external forcing signal was chosen to be sinusoidal close to the resonant frequency of the cantilever, the cantilever oscillation was found to be near sinusoidal. This is partly responsible for the gentle nature of this mode of operation. The smallness of the higher harmonics also posed questions on the applicability of dynamic-mode AFM for discerning finer features of the tip sample force profile. Moreover, for the same tip sample separation, oscillations with different amplitudes were observed, which was found to cause imaging artifacts. There was also a lack of systematic methods for the identification of the tip sample force profile, which in itself is a significant application of the AFM.

One of the significant steps in addressing these issues was that of viewing the cantilever-sample system as an interconnection of a linear-time invariant cantilever system with a nonlinear tip-sample interaction system. This viewpoint enabled significant insight into the dynamic-mode operation and greatly simplified the analysis. It also enabled the use of powerful tools from systems theory.

In dynamic-mode AFM, the cantilever is actuated by an external periodic signal. The cantilever also experiences forces due to the tip sample interaction. This force, in turn, depends on the position of the tip relative to the sample and hence is a function of the deflection of the cantilever. It is assumed that a linear time-invariant model G captures the behavior of the cantilever. Thus, G is a linear time-invariant operator that takes as input the sum of the external forcing signal $g(t)$ and the tip sample interaction force $h(t) = \phi(p(t))$. It produces the deflection signal $p(t)$ as the output (see Fig. 3). The tip sample interaction force now appears as a feedback block. In this perspective, the instantaneous tip position is fed back to the cantilever system G through the tip sample interaction system ϕ. In this way, the AFM dynamics is viewed as an interconnection of two systems, the system G, which models the cantilever, and the block ϕ which models the tip sample interaction.

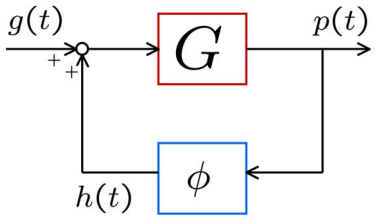

Fig. 3. Feedback perspective of dynamic-mode AFM dynamics.

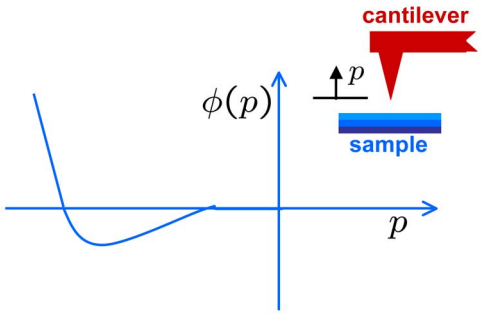

Fig. 4. Typical tip-sample interaction system ϕ, as a function of the deflection p.

The cantilever dynamics is accurately captured by a linear time-invariant multimode model described in [20]. A typical interaction force profile is depicted in Fig. 4. As described earlier, it consists of long-range attractive forces and short-range repulsive forces. Note that ϕ could be any nonlinear operator of p and need not be memoryless. For example, the interaction force could be a function of the velocity of the microcantilever tip, as in the case of dissipative samples.

The analysis of dynamic-mode operation in what follows is based on the Luré system perspective. One of the primary tools for analysis is the harmonic balance method, which is presented next. The near sinusoidal nature of the cantilever oscillation is explained using the Luré system perspective in conjunction with the harmonic balance method. The Luré perspective also lends itself to a methodical way of estimating the tip sample force profile. One strategy is to assume a parametric model of the tip sample interaction system and use the Luré structure and the harmonic balance method to identify the unknown parameters of the model.

III. Harmonic Balance Equations for Dynamic-Mode AFM

Assumptions of linear time invariance on G and time invariance on ϕ enables the use of harmonic balance techniques to study the AFM dynamics. The forcing signal g is assumed to be periodic, with period T. It is shown in [21] that under unrestrictive assumptions, a cantilever-sample system admits a periodic solution with the same period T as that of the forcing signal g. Such a periodic solution is denoted by $p^*(t)$. If the tip sample interaction force is assumed to be time invariant it follows that $h^* = \phi(p)$ is also periodic with period T. Thus, p^*, h^*, and g all admit expansions of the form $p^*(t) = \Sigma_{k=-\infty}^{\infty} p_k e^{jk\omega t}$, $h^*(t) = \Sigma_{k=-\infty}^{\infty} h_k e^{jk\omega t}$, and $g(t) = \Sigma_{k=-\infty}^{\infty} g_k e^{jk\omega t}$, where p_k, h_k, and g_k are the exponential Fourier coefficients of p^*, h^*, and g, respectively, and $\omega = 2\pi/T$. On the periodic orbit, Fig. 3 can be viewed as Fig. 5. Given the linear time invariance of G, it follows that

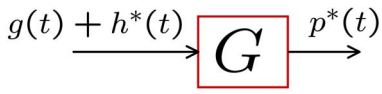

Fig. 5. Relationship between the periodic signals $g(t)$, $p^*(t)$, and $h^*(t)$.

$$G(jk\omega)(g_k + h_k) = p_k, \qquad \text{for all } k = 0, \pm 1, \pm 2, \ldots. \quad (1)$$

Equation (1) constitutes the harmonic balance equations that need to be satisfied by the cantilever sample system. Over the years, several schemes have been developed to identify G in a precise manner [20], [22]. The Fourier coefficients of the forcing signal g_k are known and those of the cantilever oscillations p_k can be obtained from measurements. The harmonic balance equations can then be used to evaluate h_k, the Fourier coefficients corresponding to the tip sample interaction force signal

$$h_k = G^{-1}(jk\omega)p_k - g_k. \quad (2)$$

A. Model for Tip Sample Interaction Force and Its Identification

Harmonic balance equations serve as powerful tools for the identification of tip sample interaction force models. The Fourier coefficients of the tip sample interaction force signal h_k can be processed to provide information on the sample properties that can be used to identify various parameters in a given model of the tip sample interaction force. An approach to identifying the tip sample interaction is to assume a parametric model that takes in as input the tip displacement and provides the force on the cantilever due to the sample as its output. Let $\phi(\Theta)$ denote such a model, where Θ is a finite set of parameters. Thus, we have $\phi(p(t)) = \phi(\Theta)[p(t)]$. The corresponding minimization problem is

$$\min_{\Theta} \Sigma_{k=-\infty}^{\infty} |\phi_k - h_k|^2 \quad (3)$$

where ϕ_k are the Fourier coefficients of $\phi(\Theta)[p(t)]$. Note that the tractability of the problem depends on the parametric model ϕ. One such parametric model is a simple piecewise linear model.

Fig. 6 depicts the piecewise linear model for the tip sample interaction force. It is designed to capture the tip sample force profile that has long-range attractive and short-range repulsive components. The former is modeled by a negative spring denoted by $-\omega_a^2$; the latter by a positive spring denoted by ω_b^2. The dissipation in the sample is captured by a damper denoted by δ. The distance between the unforced cantilever tip and the beginning of the repulsive regime l is a good measure of the cantilever sample offset. The length of the attractive regime is denoted by d. The various parameters of this simple tip sample interaction model could be identified using the harmonic balance method. The details of the identification procedure, which also uses the

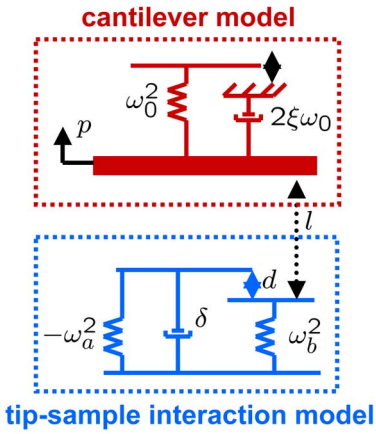

Fig. 6. Tip sample interaction model and single-mode model for the cantilever.

power balance equations, are provided in [9]. The identification scheme is revisited in the experimental part of Section IV.

B. Dominance of the First Harmonic

The Luré system perspective combined with the harmonic balance equations provides significant insights into dynamic-mode operation. In most dynamic-mode operations, the forcing signal is a single sinusoid with a frequency close to the resonant frequency of the first mode of the cantilever. If the forcing frequency is selected to be the resonant frequency, then, assuming that the dynamics of the cantilever is well captured by the single-mode approximation, it is seen that $|G(jk\omega)| \approx 0$ for $k = 2, 3, \ldots$. Thus, G acts like a low-pass filter that ensures that the higher-frequency components get filtered. From the harmonic balance equations, it immediately follows that $p_k \approx 0$ if $|k| \geq 2$. This explains the fact that in typical dynamic-mode operation the microcantilever oscillation is near sinusoidal or, in other words, the first harmonic is the predominant component of the cantilever oscillation. Regardless of whether the tip sample interaction force signal consists of higher harmonics, the measurable deflection signal is dominated by the first harmonic. A more detailed analysis of the generation of higher harmonics and bounds on their magnitude is referred to a later section. Typical imaging applications utilize the amplitude and phase of the first harmonic. Hence, the relationship between the first harmonic and the cantilever sample offset has to be well understood. The transient behavior of the amplitude and the phase is also of interest as it influences the imaging bandwidth.

IV. Analysis of the First Harmonic

In this section, a detailed analysis of the first harmonic is presented. A first-mode approximation is sufficient to capture the cantilever dynamics when analyzing the first harmonic. In the subsequent analysis, all parameters are normalized to the mass of the cantilever. In accordance with the Luré perspective, G is given by $1/(s^2 + 2\xi\omega_0 s + \omega_0^2)$ and the tip sample interaction system is denoted by ϕ.

The deflection signal $p(t)$, is governed by

$$\ddot{p} + 2\xi\omega_0\dot{p} + \omega_0^2 p = g(t) + \phi(p, \dot{p}). \tag{4}$$

The tip encounters the tip sample interaction forces towards the end of the negative cycle of the oscillation. Thus, during most of the oscillation cycle the tip does not interact with the sample. This motivates the analysis using the asymptotic methods developed for weakly nonlinear systems. If $g(t) = \gamma\cos\omega t$, then it can be shown that the solution of the dynamics is given by

$$p(t) = a\cos(\omega t + \theta) \tag{5}$$

where the slowly varying variables, the *amplitude* a, and the *phase* θ are dictated by (see [13] and [19])

$$\dot{a} = -\frac{\delta_e(a)}{2}a - \frac{\gamma\sin\theta}{\omega_0 + \omega} \tag{6}$$

$$\dot{\theta} = \omega_e(a) - \omega - \frac{\gamma\cos\theta}{a(\omega_0 + \omega)} \tag{7}$$

$$\omega_e^2(a) = \omega_0^2 - \frac{2}{a}\overline{\phi}_c \tag{8}$$

$$\delta_e(a) = 2\xi\omega_0 + \frac{2}{a\omega}\overline{\phi}_d \tag{9}$$

where

$$\overline{\phi}_c = \frac{1}{2\pi}\int_0^{2\pi}\phi(a\cos\psi, -a\omega\sin\psi)\cos\psi d\psi \tag{10}$$

$$\overline{\phi}_d = \frac{1}{2\pi}\int_0^{2\pi}\phi(a\cos\psi, -a\omega\sin\psi)\sin\psi d\psi. \tag{11}$$

If the sample is conservative, the dissipative component of the tip sample interaction, $\overline{\phi}_d = 0$, and $\overline{\phi}_c$ does not depend on the phase θ. Note that near resonance excitation is necessary for the validity of this analysis. Let $\Delta\omega_e^2 = (2/a)\overline{\phi}_c$ and $\Delta\delta_e = (2/a\omega)\overline{\phi}_d$. From (9), $\Delta\delta_e$ is the difference between the equivalent damping of the cantilever sample system and the damping of the cantilever alone. Hence, it is a measure of the dissipative component of the tip sample interaction. Similarly, from (8), $\Delta\omega_e^2$ is a measure of the conservative interaction and can take positive or negative values depending on $\overline{\phi}_c$.

A. Multivalued Frequency Response

For a fixed cantilever sample offset l (which translates to a fixed tip sample interaction ϕ) and a fixed frequency of forcing ω, the amplitude a, and phase θ [the quantities defined by (5)] evolve according to (6) and (7). It can be shown from (6) and (7) that each fixed point for the amplitude and phase dynamics has to satisfy the relation

$$a^2\left\{\left(\omega_e(a)^2 - \omega^2\right)^2 + 4\omega^2\delta_e(a)^2\right\} = \gamma^2. \tag{12}$$

Hence, for each fixed l (hence a fixed tip sample interaction potential) and ω, there could be more than one equilibrium point. If one has a plot of the fixed-point amplitudes versus the frequency of forcing, then it can be shown that a particular fixed-point amplitude a_0 is stable if

$$\left.\frac{da}{d\omega}\right|_{a=a_0} > , \quad \text{if} \quad \omega_e(a)^2 > \omega^2 + 2\delta_e(a)^2$$
$$\leq 0, \quad \text{if} \quad \omega_e(a)^2 < \omega^2 + 2\delta_e(a)^2. \tag{13}$$

If the damping is very small, then a fixed-point amplitude is stable if the slope $da/d\omega$ at that point is positive for forcing frequencies below the equivalent resonant frequency corresponding to that amplitude $(\omega_e(a))$. This is also true when the slope $da/d\omega$ is negative for forcing frequencies above the equivalent resonant frequency.

For a fixed-cantilever sample offset and a fixed-forcing frequency, let (a_0, θ_0) be an equilibrium point of the dynamical equations (6) and (7). Then the steady-state periodic solution of the cantilever-sample system is given by $p^*(t) = a_0 \cos(\omega t + \theta_0)$ and the steady-state tip sample interaction force signal is $h^*(t) = \phi(a_0 \cos(\omega t + \theta_0), -a_0\omega \sin(\omega t + \theta_0))$. Let h_1 be the first Fourier coefficient of the signal $h(t)$. Then, from the expression for $\overline{\phi}_c$ (9), it can be shown that $\overline{\phi}_c = h_{1r} \cos\theta_0 + h_{1i} \sin\theta_0$. Similarly from the expression for $\overline{\phi}_d$ (8), $\overline{\phi}_d = h_{1r} \sin\theta_0 - h_{1i} \cos\theta_0$, where h_{1r} and h_{1i} are the real and imaginary parts of h_1. Hence, the conservative and dissipative components of the tip sample interaction force are directly linked to the first Fourier coefficient of the steady-state tip sample interaction force signal, which can be measured using the harmonic balance equations (2) described in Section III.

B. Experimental Validation

The analytical results presented are further illustrated by an experiment using a silicon cantilever, AC160TS from *Olympus*, with natural frequency 335.4 kHz. The length, width, and thickness are 160, 50, and 4.6 μm, respectively, and the spring constant is 42 N/m. The quality factor is measured to be 170.

The cantilever is oscillated at the resonant frequency $f_0 =$ 335.4 kHz to an amplitude of 24.25 nm. The sample [highly oriented pyrolitic graphite (HOPG)] is moved towards the freely oscillating cantilever and then away. Approach and retraction of the sample are performed sufficiently slow so that the amplitude and phase evolving according to (6) and (7) settle to an equilibrium amplitude and phase for a particular cantilever sample offset. The resulting amplitude a is plotted against the cantilever sample offset l [see Fig. 7(a)]. Using the harmonic balance equations and the identification schemes described in [9], the parameters for the tip sample interaction-force model, ω_a, ω_b, δ, and d were estimated for the experimental data: $\omega_a = 0.765\ \mu s^{-1}$, $\omega_b = 3\ \mu s^{-1}$, $\delta = 0.012\ \mu s^{-1}$, and $d = 2.55$ nm (see Fig. 6). Using these parameters, simulations were performed and the resulting amplitude versus cantilever sample offset data is compared with the experimental results in Fig. 7(a). The remarkable similarity between the experimental and the simulated data confirm the capability of the simple piecewise linear tip sample interaction model to capture the first harmonic behavior.

To simplify the discussion on the stability of equilibrium points, the damping term δ is assumed to be zero in the model. This entails some discrepancy with the experimental data as shown in Fig. 7(b). However, there still is a good qualitative match showing the discontinuous jumps. Fig. 8 depicts the multivalued frequency response plot for a cantilever sample offset of 23 nm obtained using the piecewise linear model. It also shows the equivalent resonant frequency $\omega_e(a)$ plotted as a function of the amplitude. For the forcing frequency, which is equal to the free resonant frequency of the cantilever, there are three fixed points X, Y, and Z. From the stability criteria developed earlier, the fixed points X and Z are stable, whereas Y is unstable.

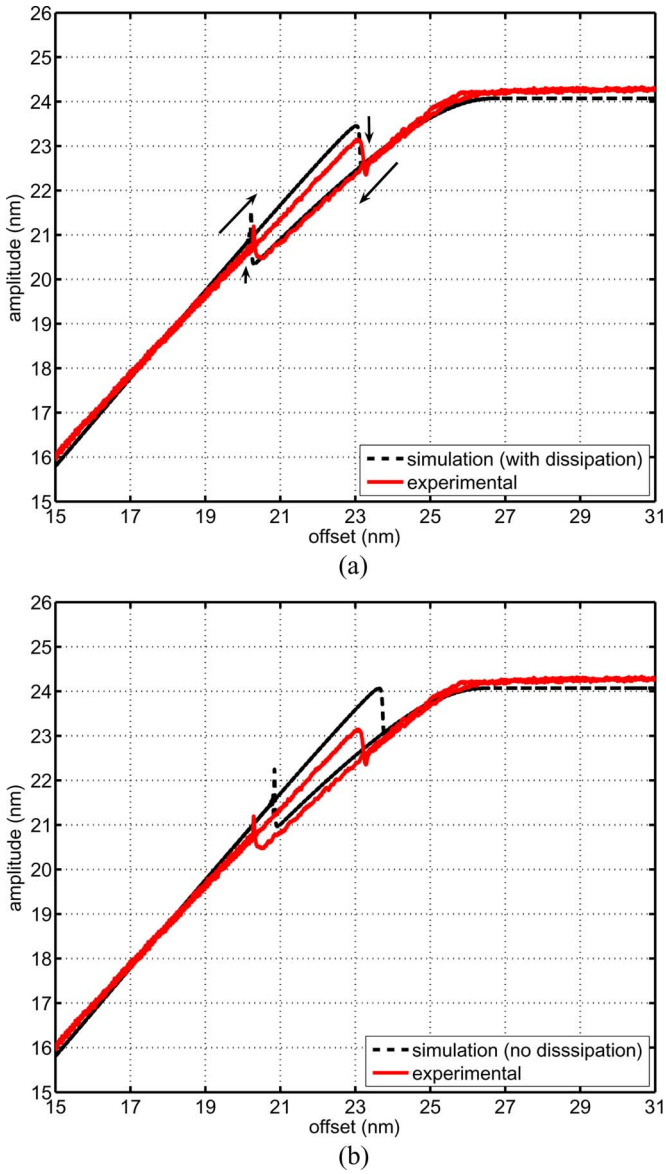

Fig. 7. (a) Comparison of the amplitude versus cantilever sample offset curve obtained using the interaction model with that obtained from the experiment. (b) The same comparison assuming the sample conservative.

The amplitude versus cantilever sample offset plot can be explained in terms of the multivalued frequency response plots, the resulting multiple equilibrium amplitudes and their stability. Fig. 9(a)–(e) depict the multivalued amplitude frequency plots for various cantilever sample offsets characterized by l obtained using the piecewise linear model. In these plots, the forcing frequency is depicted by the vertical line at 335.4 kHz, and the value of l that denotes the cantilever sample offset is indicated by the horizontal line. In Fig. 9(f), the amplitude versus cantilever sample offset curve is shown. In Fig. 9(a), the cantilever is freely oscillating, with $l = 30$ nm. In the approach phase, the cantilever is brought closer to the sample. As l is reduced to 24.5 nm [see Fig. 9(b)], there is only one possible fixed point denoted by B. It is also evident that the cantilever does not explore the repulsive region as the amplitude is smaller than l. As the cantilever sample offset is further reduced with $l = 23.9$ nm, there are two possible fixed points, C and J. However, the amplitude takes the value corresponding to C as the operating region is in its basin

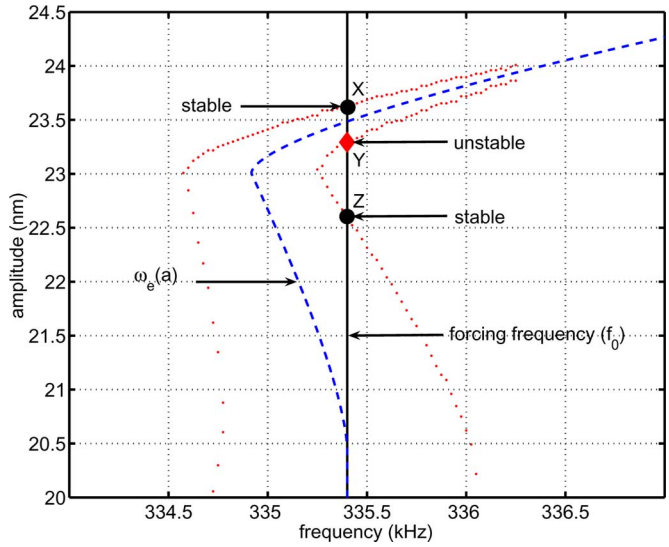

Fig. 8. Multivalued frequency response curve is shown for the cantilever sample system with a cantilever sample offset of $l = 23$ nm.

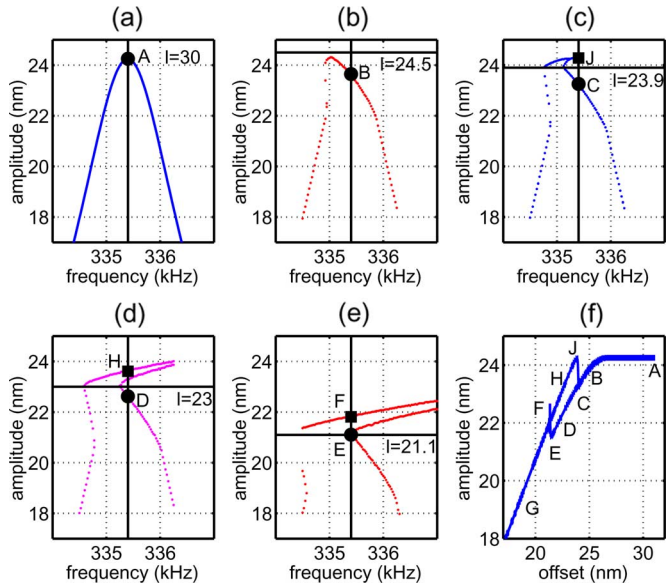

Fig. 9. (a)–(e) For different cantilever sample offsets, the multivalued frequency response curves are obtained by solving (12). (f) The discontinuities in the amplitude versus cantilever sample offset plot can be explained using the multivalued frequency response plots, the resulting multiple equilibrium amplitudes and their stability.

of attraction. With further reduction of l to 23 nm and later to 21.1 nm, the amplitude takes the values corresponding to D and E, respectively. Any further reduction of the cantilever sample offset leads to the scenario where there is only one intersection point of the vertical line with the amplitude frequency plot. Thus, the amplitude jumps to F. Note that throughout the traversal ABCDE, the tip does not interact with the repulsive part of the regime (l is greater than the amplitude). At F, the amplitude is bigger than l and thus the tip explores the repulsive part at this operating condition. Any further reduction of l leads to a single fixed-point scenario and the path FG is traversed by the tip [see Fig. 9(f)]. In the retract phase, first the path GF is traversed. In this phase, the amplitude at $l = 23$ and 23.9 nm settles to the value corresponding to points H and J, respectively. As the tip is further retracted to a value slightly greater than $l = 23.9$ nm, the tip has to take the value close to the one marked by C. Throughout the traversal GFHJ, the tip explores the repulsive part of the interaction. Thus, in the approach phase the path traversed is ABCDEFG, where during ABCDE the tip does not interact with the repulsive region. In the retract phase, the tip traverses the path GFHJCBA, where during CBA the tip again does not interact with the repulsive part.

It is quite remarkable that the first harmonic behavior is well captured by a relatively simple piecewise linear model of the tip sample interaction that accounts for the repulsive and attractive parts of the interaction and a spring-mass-damper model of the cantilever. For all imaging methods that use only the first harmonic, the first-mode approximation to the cantilever dynamics combined with the piecewise linear model for the tip sample interaction force can be used effectively to simulate the dynamic-mode AFM that can aid controller design without carrying out extensive experiments. Thus we are led to the study of higher harmonics, which have the potential to provide finer details of the tip sample interaction potential.

V. Analysis of the Higher Harmonics

In Section IV, it was shown that the first harmonic of the deflection signal is well characterized by a first mode model of the cantilever and a simple tip sample interaction force model. Even though the simplicity of the analysis is pleasing, it also points to the limitations of the first harmonic in probing intricate features of the tip sample interaction force. It is clear that the more intricate features of the tip sample force profile cannot be discerned using the first harmonic alone. This has motivated several groups to investigate and utilize the higher harmonics [23]–[27]. Proksch started using forcing frequencies with more than one harmonic to further enhance the higher harmonics [28].

The Luré system perspective is particularly well-suited for the analysis of the higher harmonics. Clearly, the harmonic balance equations introduced earlier serve as powerful tools for the study of the higher harmonics. It was shown that the bandpass characteristic of the cantilever transfer function is responsible for the predominance of the first harmonic. Even though higher harmonics of the interaction force signal are generated, they are filtered by the cantilever transfer function. Hence, it is expected that the higher harmonics close to the higher modes of the cantilever transfer function are likely to be the predominant higher harmonics. This also points to the possibility of directed design of the cantilever transfer function such that the higher harmonics of interest are allowed to pass through [29].

Besides the harmonic balance approach, a frequency-domain characterization of the nonlinear tip sample interaction system using the notion of integral quadratic constraints (IQC) could be employed for a complete frequency-domain analysis. Note that no complete characterization of the tip sample nonlinearity is available and often is the objective of the interrogation process. However, coarse characteristics of the nonlinearity can be assumed. For example, one can assume that the tip sample nonlinearity being explored in a particular operation explores the nonlinearity only in a particular sector. By assuming a sector bound, which is a coarse characterization of the nonlinearity, bounds on higher harmonics can be derived [30]. It has been shown that whereas the tip probes the net attractive regime of

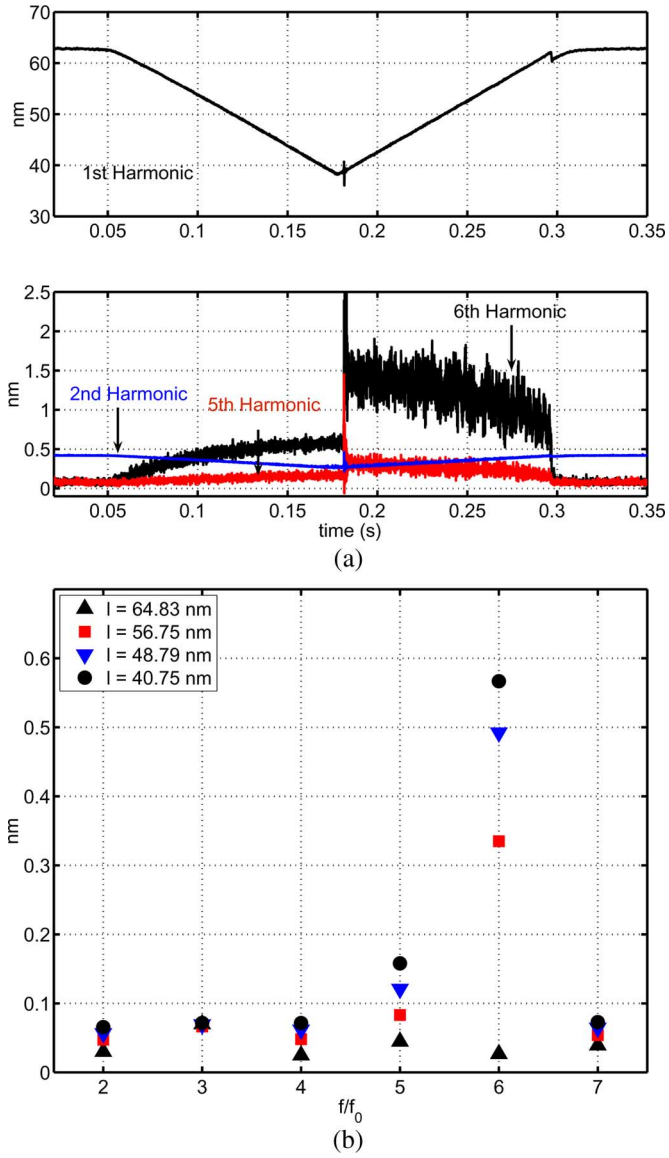

Fig. 10. (a) Experimentally obtained first, second, fifth, and sixth harmonics of the cantilever oscillation during the approach and retract of the sample towards the tip. (b) Magnitude of the first seven higher harmonics as the sample approaches the cantilever for different values of cantilever sample offset.

the tip sample interaction force, bounds on the generation of the higher harmonics can be obtained by using the cantilever frequency response and an IQC characterization of the tip sample interaction system [31], [32].

An experiment is presented that illustrates the generation of the higher harmonics. An AFM is operated in the dynamic mode using a silicon cantilever (AC240TS from *Olympus*) of length 240 μm, width 30 μm, thickness 2.7 μm, and spring constant 2 N/m. The first and second modal frequencies of the cantilever are at $f_0 = 69.1$ kHz and $f_1 = 403$ kHz, respectively. The sample (HOPG) initially is sufficiently far from the cantilever. In Section IV, the existence of two stable equilibrium points for the same cantilever sample offset was shown, one corresponding to a low amplitude oscillation and the other to a high amplitude oscillation. While describing the experimental results, it was shown that during the low-amplitude oscillation state, the tip explores only the net attractive regime of the

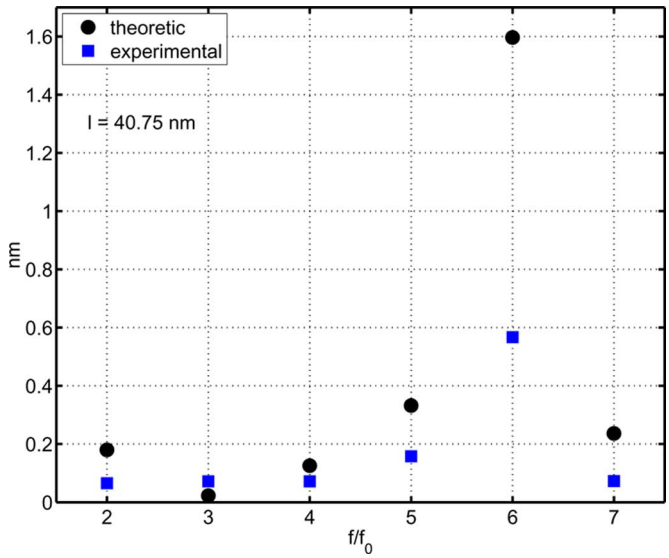

Fig. 11. For a cantilever sample offset of 40.75 nm, the theoretical bounds on the harmonics are compared with the experimental values obtained.

tip sample interaction force. It was also shown that in the high-amplitude oscillation state, it explores the net repulsive regime along with the attractive regime. This assumption had also been validated by numerical simulations and results from [24], [26], and [33]. Next, the sample is progressively moved towards the cantilever and then away from the cantilever to obtain deflection signals from the cantilever while it oscillates in the two different oscillation states. From the deflection data, the magnitudes of the harmonics of the cantilever oscillation are obtained as a function of time. The variations of the first, second, fifth, and sixth harmonic are depicted in Fig. 10(a). While approaching the sample surface, the magnitude of the first harmonic reduces with a reduction in the cantilever sample offset. It is seen in Fig. 10(a) that for a certain cantilever sample offset, the first harmonic exhibits a discontinuous jump to a higher value and stays there until it jumps back to a lower value for a larger cantilever sample offset. These are the two oscillation states of the cantilever. The higher harmonics increase with shrinking cantilever sample offset, possibly because the fraction of the period in which the cantilever interacts with the nonlinearity increases with reducing cantilever sample offset.

As expected from the preceding discussion, the harmonics close to the modal frequencies of the cantilever are particularly dominant. As Fig. 10(a) shows, the fifth and sixth harmonics are especially sensitive to the reducing cantilever sample offset. Another interesting aspect is the sudden increase in the magnitude of the fifth and sixth harmonics at the onset of high-amplitude oscillation. From the sampled deflection data, the magnitudes of the first seven higher harmonics are obtained for different cantilever sample offsets in the region where the tip is believed to be exploring the net attractive regime [see Fig. 10(b)], i.e. while the cantilever is oscillating in the low-amplitude state. Fig. 11 compares the theoretic bounds on the harmonics obtained using the IQC approach with those measured experimentally for a representative cantilever sample offset of 40.75 nm. The theoretical bounds serve as a good upper bound for the experimental measurements.

VI. Conclusion

The dynamics of the atomic force microscope operating in the dynamic mode is particularly challenging because the cantilever tip traverses a long range of nonlinear tip sample interaction forces. By viewing the dynamics as an interconnection of a linear cantilever system with a nonlinear tip sample interaction system, powerful tools from systems theory could be used to analyze the dynamics. Harmonic balance techniques provide significant insight into the steady-state behavior of dynamic-mode operation and a paradigm for the systematic identification of models of tip sample interaction as well as insights into the predominance of the first harmonic. Asymptotic methods are used to analyze the predominant first harmonic and the equations describing the evolution of amplitude and phase are presented. The transient behavior of dynamic-mode operation is captured by these equations. The steady-state values for amplitude and phase are given by the fixed points of these amplitude phase dynamical equations. The stability conditions for these equilibrium points are presented. An important insight obtained in this study is that a simple piecewise linear model is capable of reproducing most of the experimentally observed intricate features. This representative and tractable model of the tip sample interaction force can effectively be used to simulate the dynamic-mode AFM, which can aid controller design and provide insights into the AFM dynamics. To provide finer details of the tip-sample interaction, the higher harmonics have to be investigated, for which the Luré system perspective is particulary well suited. The harmonic balance method provides significant insights into the generation of the higher harmonics. Another powerful method for characterizing the higher harmonics is the frequency-domain characterization of the nonlinear tip-sample interaction system using IQCs.

Acknowledgment

The authors would like to thank J. Cleveland from Asylum Research and S. Salapaka from the University of Illinois for their fruitful discussions. They would also like to thank C. Bolliger for her assistance with the preparation of this manuscript.

References

[1] G. Binnig, C. Quate, and C. Gerber, "Atomic force microscope," *Phys. Rev. Lett.*, vol. 56, no. 9, pp. 930–933, 1986.

[2] R. Wiesendanger, *Scanning Probe Microscopy and Spectroscopy*. Cambridge, U.K.: Cambridge Univ. Press, 1994.

[3] S. Salapaka, M. Dahleh, and I. Mezic, "On the dynamics of a harmonic oscillator undergoing impacts with a vibrating platform," *Nonlinear Dyn.*, vol. 24, pp. 333–358, 2001.

[4] S. Hu and A. Raman, "Chaos in atomic force microscopy," *Phys. Rev. Lett.*, vol. 96, p. 036107, 2006.

[5] D. Sahoo, A. Sebastian, and M. V. Salapaka, "Transient-signal-based sample-detection in atomic force microscopy," *Appl. Phys. Lett.*, vol. 83, no. 26, pp. 5521–5523, 2003.

[6] A. Gannepalli, A. Sebastian, J. Cleveland, and M. V. Salapaka, "Thermally driven non-contact atomic force microscopy," *Appl. Phys. Lett.*, vol. 87, p. 111901, 2005.

[7] T. De, P. Agarwal, D. R. Sahoo, and M. V. Salapaka, "Real time detection of probe loss in atomic force microscopy," *Appl. Phys. Lett.*, vol. 89, p. 133119, 2006.

[8] A. Sebastian, M. V. Salapaka, D. J. Chen, and J. P. Cleveland, "Harmonic analysis based modeling of tapping-mode AFM," in *Proc. Amer. Control Conf.*, 1999, pp. 232–236.

[9] A. Sebastian, M. V. Salapaka, D. J. Chen, and J. P. Cleveland, "Harmonic and power balance tools for tapping-mode atomic force microscope," *J. Appl. Phys.*, vol. 89, no. 11, pp. 6473–6480, 2001.

[10] M. Stark, R. W. Stark, W. M. Heckl, and R. Guckenberger, "Inverting dynamic force microscopy: From signals to time-resolved interaction forces," *Proc. Nat. Acad. Sci.*, vol. 99, no. 13, pp. 8473–8478, 2002.

[11] R. W. Stark, G. Schitter, M. Stark, R. Guckenberger, and A. Stemmer, "State-space model of freely vibrating and surface-coupled cantilever dynamics in atomic force microscopy," *Phys. Rev. B*, vol. 69, no. 8, p. 085412, 2004.

[12] S. Hu, S. Howell, A. Raman, R. Reifenberger, and M. Franchek, "Frequency domain identification of tip-sample van der waals interactions in resonant atomic force microcantilevers," *J. Vib. Acoust.*, vol. 126, no. 3, pp. 343–351, 2004.

[13] N. N. Bogoliubov and Y. A. Mitropolskii, *Asymptotic Methods in the Theory of Non-Linear Oscillations*. New Delhi, India: Hindustan, 1961.

[14] L. Wang, "Analytical descriptions of the tapping-mode atomic force microscopy response," *Appl. Phys. Lett.*, vol. 73, no. 25, pp. 3781–3783, 1998.

[15] M. Gauthier and M. Tsukada, "Damping mechanism in dynamic force microscopy," *Phys. Rev. Lett.*, vol. 85, no. 25, pp. 5348–5351, 2000.

[16] S. I. Lee, S. W. Howell, A. Raman, and R. Reifenberger, "Nonlinear dynamics of microcantilevers in tapping mode atomic force microscopy: A comparison between theory and experiment," *Phys. Rev. B*, vol. 66, p. 115409, 2002.

[17] A. S. Paulo and R. Garcia, "Unifying theory of tapping-mode atomic-force microscopy," *Phys. Rev. B*, vol. 66, p. 041406, 2002.

[18] R. W. Stark, G. Schitter, and A. Stemmer, "Tuning the interaction forces in tapping mode atomic force microscopy," *Phys. Rev. B*, vol. 68, p. 085401, 2003.

[19] A. Sebastian, A. Gannepalli, and M. V. Salapaka, "The amplitude phase dynamics and fixed points in tapping-mode atomic force microscopy," in *Proc. Amer. Control Conf.*, 2004, pp. 2499–2504.

[20] M. V. Salapaka, H. S. Bergh, J. Lai, A. Majumdar, and E. McFarland, "Multimode noise analysis of cantilevers for scanning probe microscopy," *J. Appl. Phys.*, vol. 81, no. 6, pp. 2480–2487, 1997.

[21] M. V. Salapaka, D. Chen, and J. P. Cleveland, "Linearity of amplitude and phase in tapping-mode atomic force microscopy," *Phys. Rev. B*, vol. 61, no. 2, pp. 1106–1115, 2000.

[22] M. Stark, R. Guckenberger, A. Stemmer, and R. W. Stark, "Estimating the transfer function of the cantilever in atomic force microscopy: A system identification approach," *J. Appl. Phys.*, vol. 98, p. 114904, 2005.

[23] U. Dürig, "Conservative and dissipative interactions in dynamic force microscopy," *Surf. Interf. Anal.*, vol. 27, pp. 467–473, 1999.

[24] M. Stark, R. W. Stark, W. M. Heckl, and R. Guckenberger, "Spectroscopy of the anharmonic cantilever oscillations in tapping-mode atomic force microscopy," *Appl. Phys. Lett.*, vol. 77, p. 3293, 2000.

[25] R. W. Stark, "Spectroscopy of higher harmonics in dynamic atomic force microscopy," *Nanotechnol.*, vol. 15, pp. 347–351, 2004.

[26] S. Crittenden, A. Raman, and R. Reifenberger, "Probing attractive forces at the nanoscale using higher-harmonic dynamic force microscopy," *Phys. Rev. B*, vol. 72, p. 235422, 2005.

[27] F. J. Giessibl, "Higher-harmonic atomic force microscopy," *Surf. Interf. Anal.*, vol. 38, pp. 1696–1701, 2006.

[28] R. Proksch, "Multifrequency, repulsive-mode amplitude-modulated atomic force microscopy," *Appl. Phys. Lett.*, vol. 89, p. 113121, 2006.

[29] O. Sahin, C. F. Quate, O. Solgaard, and A. Atalar, "Resonant harmonic response in tapping-mode atomic force microscopy," *Phys. Rev. B*, vol. 69, p. 165416, 2004.

[30] A. Megretski and A. Rantzer, "Harmonic analysis of nonlinear and uncertain systems," in *Proc. Amer. Control Conf.*, 1998, pp. 3654–3658.

[31] A. Sebastian and M. V. Salapaka, "Analysis of periodic solutions in tapping-mode AFM: An IQC approach," presented at the Int. Symp. Math. Theory Netw. Syst., South Bend, IN, 2002.

[32] A. Sebastian, "Nanotechnology: A systems and control approach," Ph.D. dissertation, Dept. Electr. Comput. Eng., Iowa State Univ., Ames, 2004.

[33] T. R. Rodriguez and R. Garcia, "Tip motion in amplitude modulation (tapping-mode) atomic-force microscopy: Comparison between continuous and point-mass models," *Appl. Phys. Lett.*, vol. 80, no. 9, pp. 1646–1648, 2002.